Journal of Pharmaceutical and Biomedical Analysis 248 (2024) 116297

Contents lists available at ScienceDirect

Journal of Pharmaceutical and Biomedical Analysis

journal homepage: www.journals.elsevier.com/journal-of-pharmaceutical-and-biomedical-analysis

Short communication

Urinary drug metabolite profiling of tuberculosis treatment failure using proton nuclear magnetic resonance

Monique Opperman , Shayne Mason , Jessica van der Westhuizen , Du Toit Loots , Ilse du Preez *

Human Metabolomics, North-West University (Potchefstroom Campus), Private Bag x6001, Box 269, Potchefstroom 2531, South Africa

ARTICLE INFO

Keywords:
Drug metabolites
Urine
^{1}H NMR
Treatment failure
Tuberculosis

ABSTRACT

The underlying cause of tuberculosis (TB) treatment failure is still largely unknown. A ^{1}H NMR approach was applied to identify and quantify a subset of TB drugs and drug metabolites: ethambutol (EMB), acetyl isoniazid (AcINH), isonicotinic acid, pyrazinamide (PZA), pyrazinoic acid and 5-hydroxy-pyrazinoic acid, from the urine of TB patients. Samples were collected before, during (weeks one, two and four) and after standardised TB treatment. The median concentrations of the EMB and PZA metabolites were comparable between the samples from patients with eventually cured and failed treatment outcomes. The INH metabolites showed comparatively elevated concentrations in the treatment failure patients during and after treatment. Variation in INH metabolite concentrations couldn't be associated with the varying acetylator genotypes, and it is therefore suggested that treatment failure is influenced more so by other conditions, such as environmental factors, or individual variation in other INH metabolic pathways.

1. Introduction

Directly observed therapy short course (DOTS), the standard treatment approach for pulmonary tuberculosis (TB), consists of the co-administration of four first-line drugs: isoniazid (INH), rifampicin (RIF), pyrazinamide (PZA), and ethambutol (EMB), under supervision for at least six months [1]. Incidentally, in developing countries with a high TB prevalence (such as South Africa), up to 21 % of all drug-susceptible cases treated using this regimen, have unsuccessful (failed) treatment outcomes [1].

In a previous investigation, TB treatment failure was better characterised using a targeted metabolomics approach, comparing the urinary amino acid and acylcarnitine profiles of eventually cured and failed TB patients, during the intensive phase treatment period [2]. Similar metabolome variations were detected in both groups over the course of treatment, which were associated to a time-sensitive, drug-induced inhibition and stimulation of various metabolic enzymes. The failed treatment patient group showed an earlier onset of this sequential metabolome pattern, potentially related to variations in the activities of drug metabolising enzymes, such as N-acetyl transferase (NAT2).

To further elaborate on these findings, the current study used a ^{1}H NMR approach to identify and quantify a subset of first-line TB drugs and their metabolites in the urine samples of the same patient cohort, collected at various time-points during the course of the standard DOTS regimen.

2. Materials and methods

2.1. Participant recruitment and sample collection

Urine samples were previously collected [2] from culture-confirmed, drug susceptible pulmonary TB patients at the time of diagnosis (week zero), during DOTS treatment (after week one, two and four of commencing treatment) and two weeks post treatment completion (week 26). All patients received the same treatment regimen administered by healthcare professionals under supervision. TB patients were included in the study only if treatment adherence was observed on more than 80 % of days during the treatment period, and if they were HIV seronegative, not pregnant, nor diagnosed with any other chronic diseases, and if they provided a sample for at least three of the five sample collection time-points.

2.3. Chemicals and reagents

The NMR buffer consisted of a 150 mM potassium dihydrogen phosphate (KH_2PO_4) solution dissolved in ddH2O, with the pH adjusted

* Corresponding author.
E-mail address: Ilse.DuPreez@nwu.ac.za (I. du Preez).

https://doi.org/10.1016/j.jpba.2024.116297
Received 18 March 2024; Received in revised form 3 June 2024; Accepted 7 June 2024
Available online 10 June 2024

to 7.0. The buffer additionally contained 1 mM trimethylsilyl propionic acid (TSP) and 500 μM 2-chloropyrimidine-5-carboxylic acid as two internal standards, and 1 % sodium azide to prevent bacterial growth.

Sigma-Aldrich brand EMB (purity ≥ 99 %), isonicotinic acid (INA) (purity ≥ 98.5 %), pyrazinoic acid (POA) (purity = 99 %), and PZA (purity ≥ 99.0 %), were purchased from Merck (Darmstadt, Germany). Acetylisoniazid (AcINH) (purity ≥ 95.0 %) and 5-hydroxypyrazinoic acid (5-OH POA) (purity ≥ 98.0 %) were purchased from Biosynth®Carbosynth (Compton, United Kingdom). All standards were prepared to a final concentration of 1 mg/mL in ddH_2O and adjusted with 100 mM solutions of HCl and NaOH to a pH of 7.00 ± 0.05. These compounds were routinely available in the laboratory and forms part of our in-house NMR library.

2.4. Sample preparation

For quality control (QC) purposes, a pooled QC sample was prepared by combining 70 μL of urine from each analytical sample, and three aliquots of this QC sample were analysed with each sample batch. All urine samples, including QCs, were centrifuged (12,000 *g* for 5 min) prior to use, to remove potential solid particles. A 570 μL volume of supernatant was combined with 60 μL NMR buffer and 70 μL deuterated water (D_2O), to a final volume of 700 μL (90 % H_2O: 10 % D_2O, v/v), followed by brief mixing and centrifugation (12,000 *g* for 5 min). Hereafter, 540 μL of the buffered urine supernatant was transferred to a 5 mm NMR glass tube for spectral acquisition. Samples were randomly analysed, with QCs at beginning, middle and end, in six batches.

2.5. Acquisition of ^1H NMR spectra

One-dimensional ^1H NMR spectra, two-dimensional (2D) ^1H–^1H correlation spectroscopy (COSY) and ^1H–^1H J-resolved spectroscopy (JRES) NMR spectra, were created for the pure drug compounds, as described previously [3]. Samples were analysed at 500 MHz using a Bruker Avance™ III HD NMR spectrometer coupled with a 5 mm triple-resonance inverse (TXI) ^1H (^{15}N, ^{13}C) probe head, at a constant temperature of 300 K. The inner TXI probe coil was optimised for ^1H observation. ^1H spectra with a spectral width of 12 ppm, were acquired as 128 transients, in 64 data points, with a set acquisition time of 2.72 s. H_20 resonance pre-saturation was achieved through single-frequency irradiation during a 990 ms saturation delay, with a 90° excitation pulse of 8 μs. The NOESYgppr1d pulse program was used for NMR acquisition with an 8 μs pulse and a 4 s delay. Using Bruker Topspin (version 3.5, Rheinstetten, Germany), sample shimming was set to the TSP signal and automatically performed for each sample to the pre-defined D_2O reference signal. Further spectral processing, including Fourier transformation, baseline phasing and correction, and TSP calibration to 0.00 ppm, was done automatically. Spectral quality was confirmed through manual inspection of spectral resolution, ensuring a <1 Hz resonance line width for TSP.

2.6. Processing of spectral data

Data processing involved the extraction of informative regions within the 1D ^1H NMR spectra (in this case, the regions where distinct drug metabolite peaks were identified, according to the standards), for quantification, using Bruker AMIX (version 3.9.14). Additionally, these drug metabolite peaks were checked against healthy control samples that did not receive any treatment to confirm their absence and to exclude the possibility of interfering compound peaks present in the biological samples. TB parent drug metabolites, including INH and RIF, have been reported to be unstable in both plasma [16] and urine [17]. Additionally, RIF-derived metabolites such as 25-deacetylrifampicin and 3-formylrifampicin have also been reported to be unstable in urine [17]. Considering this, these compounds were not evaluated further in this study, as no discernible signals for these compounds were detected in the samples. A combined NMR spectra (Figure S1) and the 1D spectra for the isolated metabolite compounds detected and analyses in this study are available in the supplementary information (Figures S2-S7). The peaks selected for quantification were isolated with no limitations regarding signal overlapping. These metabolite identities were confirmed by comparing the 2D ^1H–^1H COSY and ^1H–^1H JRES NMR spectra of the standard solutions to that of the QC sample. Hereafter, metabolite quantification relative to the urine creatinine value was performed to get the final drug concentrations as mmol/mol creatinine. Table 1 summarises the signals (chemical shifts, number of H) used during quantification for each metabolite.

Table 1
Summary of signals used during ^1H NMR quantification for each isolated metabolite.

Chemical shift (ppm)	Annotation (number of H)
0.97	Ethambutol (6 H)
8.73	Acetyl isoniazid (2 H)
8.62	Isonicotinic acid (2 H)
9.08	Pyrazine carboxylic acid (2 H)
9.19	Pyrazine carboxamide (2 H)
8.12	5-OH-2-pyrazine carboxylic acid (2 H)

2.7. Data analyses

Precision was evaluated based on the laboratory coefficient of variation (CV) of the QC samples, which is the laboratory standard deviation (SD), calculated by variance components or the weighted sum of the between and within batch variability, divided by the average. Metabolites were regarded to be measured with suitable precision if the laboratory CV was less than 20 % [4]. To graphically illustrate the measured drug metabolite concentrations, box plots and line graphs were constructed using R (version 4.2.0). All conclusions were drawn from the relative compound ratio comparisons between the sample groups, as presented in the box plots.

3. Results and discussion

3.1. Population

A total of 39 patients (28 with a cured and 11 with a failed treatment outcome) were included in the study. In total 175 urine samples were analysed. Patient demographics are provided in Table 2, along with their predetermined genotypic NAT2 acetylator statuses, which formed part of a previous study [5].

3.2. Drug metabolite profiles

The metabolite concentrations detected in each sample analysed are given in the supplementary material (Table S1). All six of the drug metabolites analysed had calculated QC laboratory CV's < 20 %, indicating suitable method precision (Table S2).

Table 2
Patient cohort demographics.

Patient demographics	Cured (n=28)	Failed (n=11)
Age (Average years)	34.71 ± 10.15	39.45 ± 11.11
Gender (Male/Female)	14/14	6/5
BMI (Average kg/m^2)	18.52 ± 2.02	18.86 ± 1.73
Genotypic NAT2 acetylator status		
Slow	8 (29 %)	3 (27 %)
Intermediate	16 (57 %)	3 (27 %)
Rapid	3 (11 %)	3 (27 %)
Not recorded	1 (4 %)	2 (18 %)

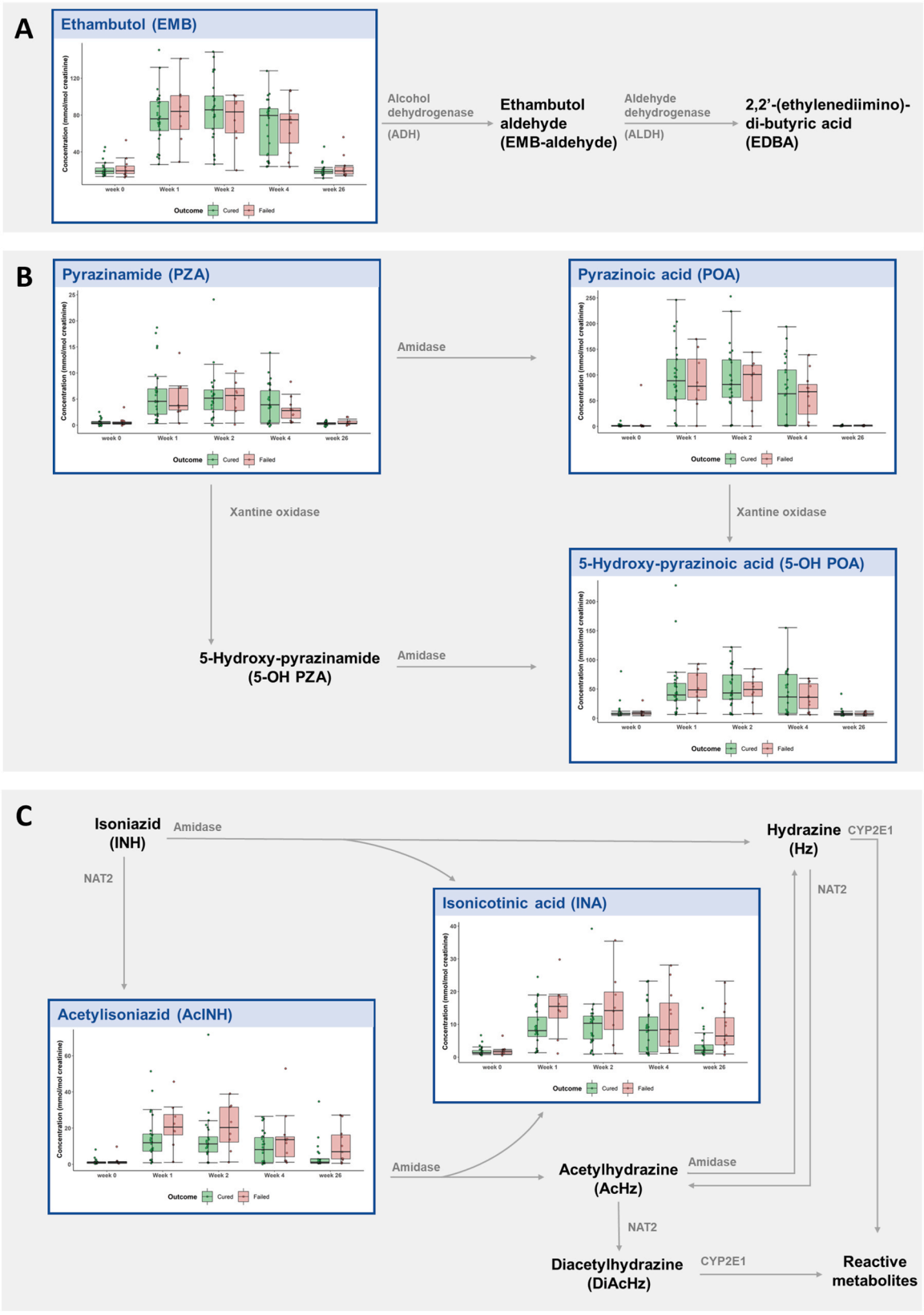

Fig. 1. EMB (A), PZA (B) and INH (C) metabolism overview, and box plots of the concentration value (mmol/mol creatinine) (y-axis) of each drug metabolite detected in the urine samples of the cured (green) and failed (red) TB patient groups before (week 0), during (after weeks 1, 2, and 4) and after treatment (week 26) (x-axis).

3.2.1. Ethambutol

Following oral administration, most of the ingested EMB is excreted in the urine, while only a small portion (roughly 8–15 %) is oxidised in the liver, yielding the inactive metabolites, EMB-aldehyde and 2,2′-(ethylenediimino)-di-butyric acid, as depicted in Fig. 1A [6].

No significant differences in the median EMB concentration between the failed and cured patient samples were observed, at any of the sample collection points (Fig. 1A), indicating a similar metabolism and excretion pattern for both the cured and failed treatment patient groups. Furthermore, no significant EMB differences were detected when comparing the four treatment weeks for either patient group, and the post treatment (week 26) drug concentrations were comparable to that measured before treatment commenced, which was virtually zero. This confirms our previous findings which could not link any of the observed time-dependent urine metabolome variation seen in TB patients with potential inconsistent EMB concentrations over the course of treatment when comparing a treatment cured to treatment failed patient sample group [2,7]. Instead, the human metabolome variation seen could only indirectly be linked to an EMB induced variation in the functioning of various enzymes, such as alcohol dehydrogenase (ADH) and cytochrome P450 (CYP) 2E1 [2].

3.2.2. Pyrazinamide

As seen in Fig. 1B, PZA is mainly metabolised via two pathways, resulting in three PZA metabolites namely, 5-OH PZA, POA and 5-OH POA, all of which are excreted through the kidneys (urine) [8]. In our study, we detected only PZA and its two metabolites, POA and 5-OH POA.

For the cured patient group, the median PZA and POA concentrations slightly declined at week four of treatment (Fig. 1B), concurring with our previous findings, using an untargeted gas chromatography-mass spectrometry approach [7]. Here, 5-OH POA, which was not detected in our previous investigations, showed a similar trend in the cured patients, and the occurrence was also seen in the failed patient group, for PZA and the two detected PZA metabolites. Although this small decline is not necessarily statistically or biologically significant, it could perhaps be ascribed to the longer half-life of PZA compared to other TB drugs, causing a slower elimination from the body and resulting in a more gradual decrease in urinary excretion rates [6]. The detected concentrations of the PZA metabolites were comparable between the two patient groups at all time-points.

3.2.3. Isoniazid

As can be seen in Fig. 1C, INH metabolism is somewhat more complex compared to the other first-line TB drugs, comprising of acetylation of roughly 50–90 % of the ingested parent drug to AcINH via NAT2 [9], followed by amidase hydroxylation of AcINH to INA and acetylhydrazine (AcHz), the latter of which can again be acetylated to diacetylhydrazine (DiAcHz) via NAT2. INH can also directly be hydrolysed via amidase to hydrazine (Hz, a potent hepatotoxin) and INA [9]. CYP2E1 further oxidises Hz and DiAcHz to produce other highly reactive hepatotoxins [10].

In contrast to ETH and PZA, a clear difference in the box plots of the INH metabolites; AcINH and INA, can be seen when comparing the cured and failed treated patient groups, with comparatively higher median concentrations in the failed cohort at most time-points during and post treatment (Fig. 1C). This coincides with our previous investigation, where the differences between the treatment-induced human urine metabolome in cured and failed patient groups were associated with the different rates of the INH metabolism. However, in the aforementioned investigation, this occurrence was ascribed to the possible variation in the NAT2 genotype (slow, intermediate, and rapid acetylators) between the treated patient groups [2]. However, in the current study, the treatment failed patient group, comprised of a uniformly distributed categorization of the NAT2 genotype status (Table 1). To further test this hypothesis, we plotted the median concentrations of AcINH and INA for each genotype, within the two sample groups (Fig. 2).

Interestingly, for both INH drug metabolites, the patient data grouped together according to treatment outcome, and not according to the NAT2 genotype, with all three acetylator groups showing higher median concentrations in the failed patient group, comparatively. We were also not able to identify a distinct pattern when observing the patient results in accordance with their different acetylator statuses, within the two patient groups, as would theoretically be expected. Given that NAT2 is a highly polymorphic gene with over 40 allelic variations, it has been suggested that the current three-class genetic categorisation presently used, may not be suitable for properly defining the enzymatic capacity of this system [10]. Furthermore, research suggests that non-genetic variables, such as drug interactions or oxidative stress conditions, may also affect NAT expression and function [11]. Consequently, environmental factors perhaps have a more prominent effect on the NAT phenotype, compared to the effect induced by the genotype. RIF induction of miRNA expression, for example, has been associated with a reduced NAT2 gene expression, possibly resulting in a drug induced

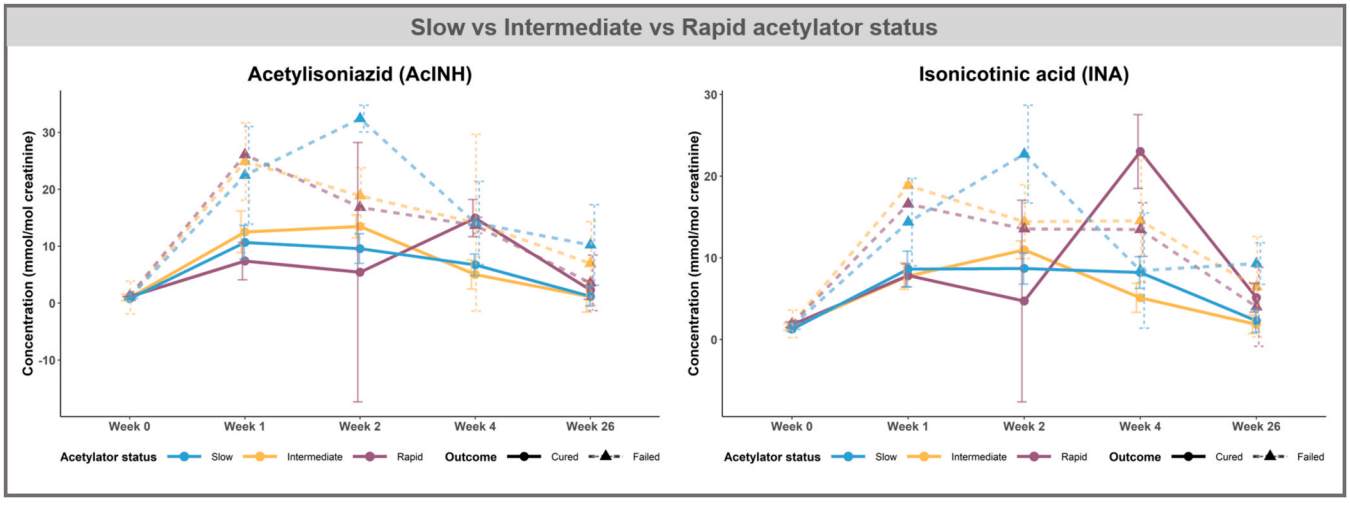

Fig. 2. Line graphs comparing the median concentration value (mmol/mol creatinine) (y-axis) of AcINH and INA with one standard error for each NAT2 genotype acetylator status (slow: blue, intermediate: yellow, rapid: purple) in the cured (solid line) and failed (dashed line) TB patient groups before (week 0), during (weeks 1, 2, and 4) and after treatment (week 26) (x-axis).

slow NAT2 phenotype, regardless of the NAT2 acetylator genotype [12]. The inter-individual variation in the metabolism of RIF, could therefore also play an important role in the INH metabolism variation seen here. Unfortunately, the current method used does not allow for the detection and quantification of RIF or its metabolites. Furthermore, in addition to the main metabolic pathways described above, INH can also be metabolised enzymatically and non-enzymatically into various other metabolites and adducts [6,13]. It is therefore possible that the variability seen between the concentrations of the INH metabolites in the cured and failed treated patients, are linked other genotypes and/or environmental conditions associated with these alternative reactions, resulting in the variations seen in the INH metabolism rates, between individuals. This speculation would also explain the relatively high INH drug metabolite concentrations detected in the failed patients at week 26, collected two weeks after treatment stopped.

4. Conclusion

Comorbidities, lifestyle, sociodemographic characteristics, and treatment-related factors (e.g., development of drug resistance or drug-related adverse effects) can all contribute to unsuccessful treatment outcomes [1]. The contribution of inter-individual genetic and metabolic variations towards the outcome of TB treatment have recently also become a topic of interest amongst researchers [6,14,15].

From our cohort, it is clear that differences exist in specifically the INH metabolism when comparing the cured and failed treatment groups. This variation could not be directly linked to the NAT2 genotypic acetylation status of the patients, and it is therefore postulated that the NAT2 phenotype might strongly be related to various other environmental factors and or alternative INH metabolic pathways, which can be investigated in the future to better understand TB treatment failure.

It is important to clarify that this study was an investigative study aimed at detecting different drug and drug related metabolite concentrations between two TB treatment outcome groups. The study had a limited cohort size. Nevertheless, it has significant implications for understanding drug metabolism, which can guide future research in validating and refining analytical methods for TB drug monitoring. Nonetheless, this study demonstrates the feasibility of using ^{1}H NMR spectroscopy for analysing TB drugs and their metabolites in urine, highlighting the potential of NMR as a non-invasive and informative tool for pharmacokinetic studies in TB patients. This study further emphasises the importance of extensive cohort classification and characterisation for the purpose of establishing more personalised research approaches.

Funding

The financial assistance of the National Research Foundation (NRF) of South Africa for this research is gratefully acknowledged (UID: 136296 and PSTD220322391). The opinions expressed and conclusions derived are those of the authors and are not necessarily those of the NRF.

Ethical statement

The study was approved by the ethics committees of Stellenbosch University (no. 99/039) and the North-West University (no. NWU-00127–11-A1–01). All participants provided written, informed consent and samples were anonymized prior to metabolomics analyses.

CRediT authorship contribution statement

Ilse Du Preez: Writing – review & editing, Supervision, Methodology, Investigation, Conceptualization. **Du Toit Loots:** Writing – review & editing, Supervision. **Jessica Van der Westhuizen:** Writing – review & editing, Formal analysis. **Shayne Mason:** Writing – review & editing, Methodology, Formal analysis. **Monique Opperman:** Writing – original draft, Visualization, Software, Methodology, Investigation, Data curation.

Declaration of generative AI and AI-assisted technologies in the writing process

During the preparation of this work the author(s) used ChatGPT (GPT-4) solely for the purpose of improving the general grammar and readability of the manuscript content. After using this tool/service, the author(s) reviewed and edited the content as needed and take(s) full responsibility for the content of the publication.

Declaration of Competing Interest

The authors declare that they have no known competing financial interests or personal relationships that could have appeared to influence the work reported in this paper.

Data availability

Data will be made available on request.

Acknowledgements

The NRF/DST Centre of Excellence for Biomedical Research at the University of Stellenbosch for collecting the patients' samples.

Supplementary materials

In the supplementary word document, the combined NMR spectra is available in Figure S1 and the 1D spectra for each isolated metabolite compounds detected for analyses in this study are available in Figures S2-S7.

The sample data is available in Table S1 and the QC lab data and laboratory CV% is available in Table S2 in the supplementary excel workbook.

Appendix A. Supporting information

Supplementary data associated with this article can be found in the online version at doi:10.1016/j.jpba.2024.116297.

References

[1] WHO, Global Tuberculosis Report 2021, Geneva, Switzerland (WHO Press), 2021.
[2] M. Opperman, D.T. Loots, M. van Reenen, K. Ronacher, G. Walzl, I. du Preez, Chronological Metabolic Response to Intensive Phase TB Therapy in Patients with Cured and Failed Treatment Outcomes, ACS Infect. Dis. 7 (2021) 1859–1869.
[3] S. Mason, C.J. Reinecke, R. Solomons, R.A. Wevers, U.F.H. Engelke, 1)H NMR spectral identification of medication in cerebrospinal fluid of pediatric meningitis, J. Pharm. Biomed. Anal. 143 (2017) 56–61.
[4] M. Kaza, M. Karaźniewicz-Łada, K. Kosicka, A. Siemiątkowska, P.J. Rudzki, Bioanalytical method validation: new FDA guidance vs. EMA guideline. Better or worse? J. Pharm. Biomed. Anal. 165 (2019) 381–385.
[5] C.J. Werely, Pharmacogenetics of Arylamine N-acetyltransferase genes in South African populations, Stellenbosch University: Stellenbosch, 2012.
[6] I. Du Preez, D.T. Loots, Novel insights into the pharmacometabonomics of first-line tuberculosis drugs relating to metabolism, mechanism of action and drug-resistance, Drug Metab. Rev. 50 (2018) 466–481.
[7] M. Combrink, I. du Preez, K. Ronacher, G. Walzl, D.T. Loots, Time-Dependent Changes in Urinary Metabolome Before and After Intensive Phase Tuberculosis Therapy: A Pharmacometabolomics Study, OMICS 23 (2019) 560–572.
[8] T.-Y. Shih, C.-Y. Pai, P. Yang, W.-L. Chang, N.-C. Wang, O.Y.-P. Hu, A Novel Mechanism Underlies the Hepatotoxicity of Pyrazinamide, Antimicrob. Agents Chemother. 57 (2013) 1685–1690.
[9] D.J. Klein, S. Boukouvala, E.M. McDonagh, S.R. Shuldiner, N. Laurieri, C.F. Thorn, R.B. Altman, T.E. Klein, PharmGKB summary: isoniazid pathway, pharmacokinetics, Pharm. Genom. 26 (2016) 436–444.
[10] K.Y. Seng, K.H. Hee, G.H. Soon, N. Chew, S.H. Khoo, L.S. Lee, Population pharmacokinetic analysis of isoniazid, acetylisoniazid, and isonicotinic acid in healthy volunteers, Antimicrob. Agents Chemother. 59 (2015) 6791–6799.

[11] F. Rodrigues-Lima, J. Dairou, J.M. Dupret, Effect of environmental substances on the activity of arylamine N-acetyltransferases, Curr. Drug Metab. 9 (2008) 505–509.
[12] B.T. Gufford, J.D. Robarge, M.T. Eadon, H. Gao, H. Lin, Y. Liu, Z. Desta, T.C. Skaar, Rifampin modulation of xeno- and endobiotic conjugating enzyme mRNA expression and associated microRNAs in human hepatocytes, Pharmacol. Res. Perspect. 6 (2018) e00386.
[13] P. Wang, K. Pradhan, X.-b Zhong, X. Ma, Isoniazid metabolism and hepatotoxicity, Acta Pharm. Sin. B. 6 (2016) 384–392.
[14] G.N. Costa, L.A. Magno, C.V. Santana, C. Konstantinovas, S.T. Saito, M. Machado, G. Di Pietro, L. Bastos-Rodrigues, D.M. Miranda, L.A. De Marco, M.A. Romano-Silva, F. Rios-Santos, Genetic interaction between NAT2, GSTM1, GSTT1, CYP2E1, and environmental factors is associated with adverse reactions to anti-tuberculosis drugs, Mol. Diagn. Ther. 16 (2012) 241–250.
[15] E.A. Lamont, A.D. Baughn, Impact of the host environment on the antitubercular action of pyrazinamide, EBioMedicine 49 (2019) 374–380.
[16] M. Karaźniewicz-Łada, K. Kosicka-Noworzyń, P. Rao, N. Modi, Y.L. Xie, S. K. Heysell, L. Kagan, New approach to rifampicin stability and first-line anti-tubercular drug pharmacokinetics by UPLC-MS/MS, J. Pharm. Biomed. Anal. 235 (2023) 115650.
[17] M. Abouzid, K. Kosicka-Noworzyń, M. Karaźniewicz-Łada, P. Rao, N. Modi, Y. L. Xie, S.K. Heysell, A. Główka, L. Kagan, Development and Validation of a UPLC-MS/MS Method for Therapeutic Drug Monitoring, Pharmacokinetic and Stability Studies of First-Line Antituberculosis Drugs in Urine, Mol 29 (2024) 1309.